

Analysis of the $^{18}\text{F}^{g,m}(d, p)^{19}\text{F}$ reactions in the rotational model

A. O. Macchiavelli, H. L. Crawford, P. Fallon, I. Y. Lee, R. M. Clark, C. M. Campbell,
M. Cromaz, C. Morse, and C. Santamaria

Nuclear Science Division, Lawrence Berkeley National Laboratory, Berkeley, California 94720, USA



(Received 26 April 2019; revised manuscript received 24 February 2020; accepted 24 March 2020; published 30 April 2020)

Spectroscopic strengths for the $^{18}\text{F}^{g,m}(d, p)^{19}\text{F}$ reactions to members of the ground-state band in ^{19}F are interpreted in the rotational model. The analysis considers two different coupling schemes, namely, the strong and decoupled limits of the particle rotor model to describe the ground and isomeric states of ^{18}F , as well as the transitions to the ground-state band in ^{19}F . Our results, obtained using Nilsson amplitudes for the neutron levels $\frac{1}{2}[220]$, $\frac{3}{2}[211]$, and $\frac{5}{2}[202]$ calculated at a deformation $\epsilon_2 = 0.32$ are in agreement with the measurements and USDB shell-model calculations.

DOI: [10.1103/PhysRevC.101.044319](https://doi.org/10.1103/PhysRevC.101.044319)

I. INTRODUCTION

The appearance of quadrupole deformation and rotational motion in light nuclei is well established and has been extensively discussed in the literature [1–3]. However, it is fair to say that in recent years the predominant framework for interpreting the structure of such light systems has been the shell model. Indeed, for light nuclei comprehensive calculations are possible within a tractable valence space, and shell-model effective interactions are available which capture very well the physics at play. Nevertheless, this does not diminish the potential insight offered by investigating experimental observables and structure information in light systems through the lens of alternative descriptions, such as the rotational model and its coupling schemes. This is particularly important as we move towards heavier systems where state-of-the-art shell-model calculations are challenged due to the limited single-particle space that can be considered, and the mean-field Nilsson approach can provide a simple yet robust framework to study deformation and related structural aspects.

In a recent measurement carried out at the ATLAS facility [4] using the HELIOS spectrometer [5], the $^{18}\text{F}(d, p)$ reaction was used to study population of final states in the ground-state rotational band in ^{19}F , including transfer from both the previously studied [6] ^{18}F ground ($I^\pi = 1^+$) state and the isomeric ($I^\pi = 5^+$) state [7]. Comparison of derived (relative) spectroscopic factors between specific initial and final states with the results of shell-model calculations within the sd shell provided an example of the single-particle and collective duality observed in the structure of atomic nuclei [2,8].

In this work we exploit this duality in an analysis of the $^{18}\text{F}(d, p)$ results in terms of the rotational model. We consider the structure of $^{18,19}\text{F}$ in terms of the levels in the Nilsson modified harmonic-oscillator (MHO) potential [9,10] originating from the sd spherical orbits and calculate the spectroscopic strengths to ^{19}F from both the ground and isomeric states following the framework reviewed in Ref. [11] (see

also Refs. [12,13] for specific examples of odd-odd nuclei). In comparing our results with both the experimental results and the shell-model values, we are able to explore how well the rotational model can capture the physics of this system and provide an interpretation that is complementary to the shell model.

II. THE STRUCTURE OF $^{18,19}\text{F}$

To begin, we consider the description of $^{18,19}\text{F}$ within the rotational coupling scheme. The interpretation of the ground-state band of ^{19}F in the rotational model was already discussed in 1957 [14,15], alongside the neighboring even-even ^{20}Ne which shows a beautiful example of the band-termination phenomenon, where a collective rotational structure ends in the (band terminating) state with all participant nucleons having aligned angular-momentum vectors to the maximum allowed by the Pauli principle [16]. We show in Fig. 1 the energy levels of the *yrast* bands of ^{20}Ne and ^{19}F . The dot-dashed line corresponds to the expression for a perfect rotor for ^{20}Ne , i.e., $E_x \approx \frac{\hbar^2}{2\mathcal{I}} I(I+1)$, compared with the data (shown in open diamonds). The approach to the band termination is seen as the lowering in energy for the two upper states as compared with the rotor extrapolation. A similar behavior is seen for ^{19}F (filled circles) for which a leading-order fit (red solid line) gives a rotational constant $A = \frac{\hbar^2}{2\mathcal{I}} = 170$ keV and a decoupling parameter, $a = 2.20 \pm 0.35$, in line with expectations for the Nilsson proton $\frac{1}{2}[220]$ level. Specifically, based on the analysis of Refs. [14,15] we expect a quadrupole deformation of $\epsilon_2 = 0.32$, for which one calculates $a = 1.96$, in good agreement with the value obtained in the leading-order fit.

The structure of the ground state in ^{18}F can be understood as a $K^\pi = 1^+$ bandhead arising from the expected parallel strong coupling of the proton and neutron $\frac{1}{2}[220]$ levels. Following the cranked shell-model results of Ref. [18], the

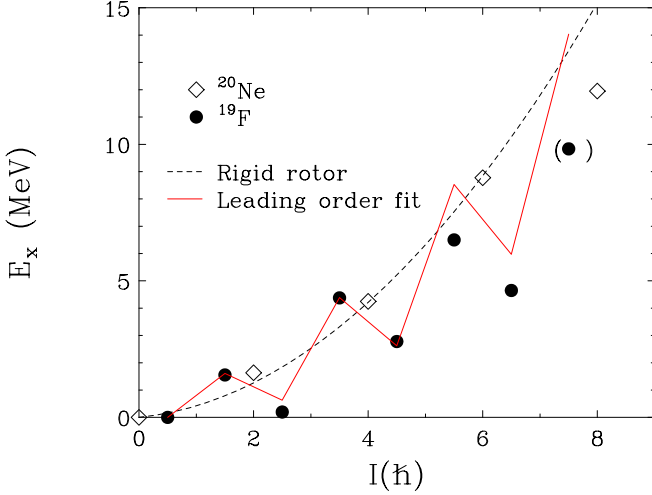


FIG. 1. Energy levels of the ground-state bands in ^{20}Ne (open diamonds) and ^{19}F (filled circles). The rigid-rotor limit for ^{20}Ne is indicated by the dashed line, while the leading-order fit for the decoupled band in ^{19}F is indicated by the solid red line. Experimental data are from Ref. [17].

higher spin members of the rotational band in ^{19}F are well described in the decoupled limit [19,20], and naturally the $I = 5^+$ isomeric state in ^{18}F can be understood as a doubly decoupled structure originating from the Coriolis-mixed Nilsson multiplet [21]. We show a schematic representation of the two coupling schemes relevant for ^{18}F (strong or parallel coupling and doubly decoupled) in Fig. 2.

The bandhead energies for the strongly coupled and decoupled structures can be simply estimated within the rotational model. For the strongly coupled 1^+ ($K = 1$) ground state we have

$$E_{1^+} \approx A + 2e_{1/2}, \quad (1)$$

where A is the rotational constant and $e_{1/2}$ is the Nilsson single-particle energy associated with the $\frac{1}{2}[220]$ level. For the doubly decoupled 5^+ state, there is no core rotation and the energy is just the contribution from the Nilsson single-particle

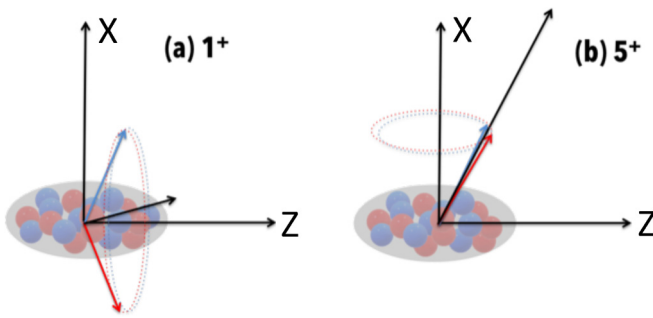


FIG. 2. Schematic representation of the structure of the (a) 1^+ ground state, corresponding to a strongly coupled configuration, and the (b) 5^+ isomeric state in ^{18}F , corresponding to a doubly decoupled configuration. The angular-momentum vectors of the neutron (blue) and proton (red) sum to the total spin of the states (black). See text for details.

energies (e_K) weighted by the fully decoupled amplitudes of each K component [taken as shown in Eq. (9)] giving

$$E_{5^+} \approx \sum_K (d_{5/2,K}^{5/2}(\pi/2))^2 2e_K. \quad (2)$$

Using $A = 177$ keV, obtained from the ^{19}F data in Fig. 1, we calculate $E_{5^+} - E_{1^+} \approx 1.14$ MeV, in good agreement with the experimental energy separation of 1.12 MeV.

III. SPECTROSCOPIC FACTORS

With the structures of $^{18,19}\text{F}$ described within the rotational framework, we can consider the calculation of spectroscopic factors for the (d, p) reaction reported in Ref. [7]. In the following, we briefly review the formalism in Ref. [11], which we have recently applied to the $N = 8$ and $N = 20$ islands of inversion [22,23]. We begin with the strong-coupling limit, applicable to transfer from the ^{18}F ground state. For the (d, p) reaction, the spectroscopic factors $S_{i,f}$ from the initial state $|I_i K_i\rangle$ to a member $|I_f K_f\rangle$ of the *yrast* band in ^{19}F can be written in terms of the Nilsson amplitudes $C_{j,\ell}$ as

$$\begin{aligned} S_{i,f}(j\ell, K) &= \frac{(2I_i + 1)}{(2I_f + 1)} \left(\langle I_i j \Omega_v K_i | I_f K_f \rangle C_{j,\ell} U_v \langle \phi_f | \phi_i \rangle \right)^2 \\ &= \frac{(2I_i + 1)}{(2I_f + 1)} \theta_{i,f}(j\ell, K)^2, \end{aligned} \quad (3)$$

where $\langle \rangle$ is the Clebsch-Gordan coefficient, U_v is the emptiness of the neutron level into which a particle is transferred, and $\langle \phi_f | \phi_i \rangle$ represents the core overlap between the initial and final states, assumed in this case to be ≈ 1 . This is a simplifying assumption, but not unreasonable, because the valence proton and neutrons outside the ^{16}O “core” are the important degrees of freedom for this reaction.

As discussed earlier, the relevant neutron level for the ground state in ^{18}F is the Nilsson orbit $\nu_{\frac{1}{2}}[220]$, which in the spherical $|j, \ell\rangle$ basis takes the form

$$|\frac{1}{2}[220]\rangle = C_{1/2,0}|s_{1/2}\rangle + C_{3/2,2}|d_{3/2}\rangle + C_{5/2,2}|d_{5/2}\rangle. \quad (4)$$

Here, $C_{j,\ell}$ are the amplitudes entering in Eq. (3). The U_v (and corresponding fullness, V_v) factors for the neutron quasiparticles are obtained by solving the relevant BCS equations [10].

The case for transfer from the isomeric state is more complicated as a result of the Coriolis K mixing in the 5^+ initial state, which gives rise to a wave function

$$\psi_I = \sum_K \mathcal{A}_K |IK\rangle. \quad (5)$$

Taking into account this expression for the initial-state wave function, Eq. (3) is modified to the form

$$S_{i,f}(j\ell) = \frac{(2I_i + 1)}{(2I_f + 1)} \left(\sum_K \mathcal{A}_K \theta_{i,f}(j\ell, K) \right)^2, \quad (6)$$

where special care should be given to the relative phases of the Nilsson amplitudes and Clebsch-Gordan coefficients entering the expression. The relevant Nilsson levels to be considered include now $\nu_{\frac{3}{2}}[211]$ and $\nu_{\frac{5}{2}}[202]$ in addition to $\nu_{\frac{1}{2}}[220]$.

TABLE I. Relative spectroscopic factors S_{expt} for levels belonging to the ^{19}F $K = 1/2^+$ band. All values are normalized to that of the 1554 keV $3/2^+$ level, as done in Ref. [7].

I_i^π	I_f^π	E_f (keV)	ℓ	S_{expt}	USDB	Nilsson
1^+	$1/2^+$	0.0	0	0.4(2)	0.64	1.1
			2			0.12
	$5/2^+$	197	2	0.6(2)	0.48	0.86
	$3/2^+$	1554	2	1	1	1
	$7/2^+$	4378	2	0.4(3)	0.39	0.33
5^+	$5/2^+$	197	2	<1	0.54	0.23
	$9/2^+$	2780	0	<0.4	0.30	0.52
			2	<1.2	0.57	0.18
	$7/2^+$	4378	2	<1.3	1.03	<0.1
	$13/2^+$	4648	2	1.8(4)	1.72	1.43
	$11/2^+$	6500	0	...	0.50	<0.1
			2	...	0.54	<0.1

Analogous to Eq. (4), the wave functions of these two levels can be written as

$$|\frac{3}{2}[211]\rangle = C_{3/2,2}|d_{3/2}\rangle + C_{5/2,2}|d_{5/2}\rangle \quad (7)$$

and

$$|\frac{5}{2}[202]\rangle = |d_{5/2}\rangle. \quad (8)$$

Because we are making the simplifying assumption that we are in the rotation-aligned coupling limit of a single- j level,¹ the amplitudes \mathcal{A}_K entering into Eq. (6) are given by the Wigner d function evaluated at $\pi/2$, the angle between the symmetry and rotation axes, i.e.,

$$\mathcal{A}_K \approx d_{5/2,K}^{5/2}(\pi/2). \quad (9)$$

IV. RESULTS

Within this established framework we calculate the spectroscopic factors in Eqs. (3) and (6) by using the Nilsson wave functions calculated at a deformation $\epsilon_2 = 0.32$ (see Sec. II) using the standard parametrization of the Nilsson MHO potential [24]:

$$|\frac{1}{2}[220]\rangle = 0.533|s_{1/2}\rangle - 0.36|d_{3/2}\rangle + 0.78|d_{5/2}\rangle \quad (10)$$

and

$$|\frac{3}{2}[211]\rangle = 0.25|d_{3/2}\rangle + 0.96|d_{5/2}\rangle. \quad (11)$$

Guided by BCS calculations, the emptiness U_ν was assumed to be 0.71 ($U_\nu^2 = 0.5$) for the $\frac{1}{2}[220]$ level at the Fermi surface, and 1 for both the $\frac{3}{2}[211]$ and $\frac{5}{2}[202]$ levels. Our results for the relative S_{if} are summarized in Table I and Fig. 3, following a similar format as that used in Ref. [7], presenting the ratio with the value for the ground state $1^+ \rightarrow 3/2^+$ transition. For comparison, we also include in Fig. 3 the results for transfers from the isomeric state assuming a

¹While Coriolis mixing of additional Nilsson levels is possible, it is expected that the contribution is small.

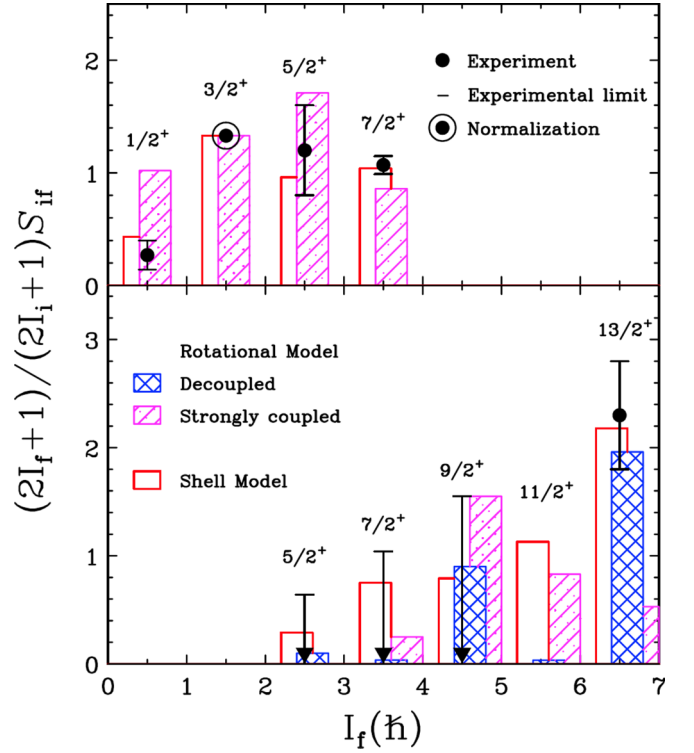


FIG. 3. Rotational model (blue double-hatched and magenta single-hatched bars) (d, p) spectroscopic strengths from the $I = 1^+$ ground state of ^{18}F (top), and $I = 5^+$ isomeric state in ^{18}F (bottom). Results are compared with the results of shell-model calculations using the USDB effective interaction (red open bars), and experimental data from Ref. [7] as indicated. The strengths are normalized to the $1^+ \rightarrow 3/2^+$ transition as indicated.

strongly coupled configuration, which clearly does not reproduce the experimental results, confirming the decoupled nature of the $I = 5^+$ isomer in ^{19}F .

However, it is interesting to point out the difference between the Nilsson calculation and the shell-model results for the population of unfavored states [18] in transfer from the isomer in the decoupled limit, which could indicate some limitations of this description for non-*yrast* states. In fact, the comparison of the strongly coupled and decoupled results may suggest an intermediate coupling as a function of angular momentum. Unfortunately, the current data provide only limits for these transitions and a higher-statistics experiment will be needed to settle the discrepancy.

To further assess the validity of the collective model, we have also calculated relative spectroscopic factors for proton stripping (pickup) reactions on (to) ^{18}O and compared them with experimental data [25,26] in Table II, showing similar agreement with the experiment.

It is also worthwhile to note that the wave functions we have considered in our calculations provide good agreement with the measured magnetic moments, as seen in Table III, which also illustrates a nice example of isospin symmetry between the ^{19}F - ^{19}Ne mirror pair.

Finally, the overall agreement found between the Nilsson calculations and experimental level properties and overlaps

TABLE II. Spectroscopic information from the $^{18}\text{O}(^3\text{He}, d)$ and $^{19}\text{F}(d, ^3\text{He})$ reactions [25,26] compared with our Nilsson calculations.

Nucleus	I_f^π	E_f (keV)	ℓ	S_{expt}	Nilsson
^{19}F	$1/2^+$	0.0	0	1	1
	$5/2^+$	197	2	1.4	2
	$3/2^+$	1554	2	0.98	0.93
	$9/2^+$	2780	4	0.07	0
^{18}O	0^+	0.0	0	1	1
	2^+	1980	2	1.4	2.14
	4^+	3549	4	0.1	0.0

gives strong support to the applicability of the rotational model, which seems to capture the relevant physics in an intuitive and simple framework complementary to large shell-model calculations. We believe this is an important benchmark as we embark in studies of quadrupole collectivity in heavier exotic systems where the shell model will inevitably reach limitations in model space.

V. CONCLUSION

The rotational model is able to describe the structure of ^{20}Ne and neighboring nuclei. In particular, several properties of the $^{18,9}\text{F}$ level schemes can be understood in terms of Nilsson quasiparticles coupled to a deformed rotor.

TABLE III. Comparison of experimental magnetic moments in ^{19}F and ^{19}Ne [27] with the Nilsson results, using $g_R = Z/A$ and $g_s = 0.95(g_s)_{\text{free}}$.

Nucleus	I^π	Experiment (μ_N)	Nilsson (μ_N)
^{19}F	$1/2^+$	2.63	2.56
	$5/2^+$	3.60	3.59
^{19}Ne	$1/2^+$	-1.89	-1.74
	$5/2^+$	-0.74	-0.87

In this work, we have interpreted spectroscopic factors obtained from $^{18}\text{F}^{g,m}(d, p)$ ^{19}F reactions using the formalism developed for studies of single-nucleon transfer reactions in deformed nuclei. We derived expressions for the spectroscopic factors in terms of the amplitudes of the deformed wave functions ($\epsilon_2 = 0.32$) for the members of the Nilsson levels from the sd shell entering in the description of both the strong and decoupled limits. Perhaps not surprisingly, the calculated spectroscopic strengths reproduce the data and are also in agreement with the shell-model calculations based on the USDB interaction, further supporting the single-particle and collective duality paradigm of nuclear structure.

ACKNOWLEDGMENTS

This material is based upon work supported by the US Department of Energy, Office of Science, Office of Nuclear Physics under Contract No. DE-AC02-05CH11231. We thank D. Santiago, C. Hoffman, B. P. Kay, and J. P. Schiffer for discussions on the experimental data.

-
- [1] J. P. Elliott, *Proc. Roy. Soc. Lond. A* **245**, 128 (1958).
[2] A. Bohr and B. R. Mottelson, *Nuclear Structure Volumes I and II* (W. A. Benjamin, Inc., Advanced Book Program; Reading, 1969 and 1975).
[3] I. Ragnarsson *et al.*, *Phys. Scr.* **24**, 215 (1981).
[4] <http://www.phy.anl.gov/atlas/index.html>
[5] A. Wuosmaa *et al.*, *Nucl. Instrum. Methods Phys. Res., Sect. A* **580**, 1290 (2007).
[6] R. L. Kozub, D. W. Bardayan, J. C. Batchelder, J. C. Blackmon, C. R. Brune, A. E. Champagne, J. A. Cizewski, U. Greife, C. J. Gross, C. C. Jewett *et al.*, *Phys. Rev. C* **73**, 044307 (2006).
[7] D. Santiago-Gonzalez, K. Auranen, M. L. Avila, A. D. Ayangeakaa, B. B. Back, S. Bottoni, M. P. Carpenter, J. Chen, C. M. Deibel, A. A. Hood *et al.*, *Phys. Rev. Lett.* **120**, 122503 (2018).
[8] A. Bohr, Nobel Lecture (1975); <https://www.nobelprize.org/uploads/2018/06/bohr-lecture-1.pdf>
[9] S. G. Nilsson, *Mat. Fys. Medd. Dan. Vid. Selsk.* **29**(16) (1955).
[10] S. G. Nilsson and I. Ragnarsson, *Shapes and Shells in Nuclear Structure* (Cambridge University Press, New York, 1995).
[11] B. Elbek and P. O. Tjøm, in *Advances in Nuclear Physics*, edited by M. Baranger and E. Vogt (Springer, Boston, MA, 1969), pp. 259–323.
[12] R. G. Lanier *et al.*, *Phys. Rev.* **178**, 1919 (1969).
[13] C. W. Reich, R. G. Helmer, R. C. Greenwood, and I. M. Maqib, *Nucl. Phys. A* **168**, 487 (1971).
[14] E. B. Paul, *Philos. Mag.* **2**, 311 (1957).
[15] B. C. Walsh and I. M. Maqib, *Nucl. Phys. A* **140**, 571 (1970).
[16] A. V. Afanasjev, D. B. Fossan, G. J. Lane, and I. Ragnarsson, *Phys. Rep.* **322**, 1 (1999).
[17] <https://www.nndc.bnl.gov/ensdf/>
[18] I. Ragnarsson, T. Bengtsson, and S. Aberg, *Proceedings of the XIX International Winter Meeting on Nuclear Physics, Bormio, Italy* (1981), p. 48.
[19] F. S. Stephens, R. M. Diamond, and S. G. Nilsson, *Phys. Lett. B* **44**, 429 (1973).
[20] F. S. Stephens, *Rev. Mod. Phys.* **47**, 43 (1975).
[21] A. J. Kreiner, *Z. Phys. A: At. Nucl.* **288**, 373 (1978), and references therein.
[22] A. O. Macchiavelli *et al.*, *Phys. Rev. C* **96**, 054302 (2017).
[23] A. O. Macchiavelli, H. L. Crawford, C. M. Campbell, R. M. Clark, M. Cromaz, P. Fallon, M. D. Jones, I. Y. Lee, and M. Salathe, *Phys. Rev. C* **97**, 011302(R) (2018).
[24] S. E. Larsson, G. Leander, and I. Ragnarsson, *Nucl. Phys. A* **307**, 189 (1978).
[25] L. L. Green, C. O. Lennon, and I. M. Maqib, *Nucl. Phys. A* **142**, 137 (1970).
[26] G. Th. Kaschl *et al.*, *Nucl. Phys. A* **155**, 417 (1970).
[27] N. J. Stone, *At. Data Nucl. Data Tables* **90**, 75 (2005).